Superconducting phase-locked local oscillator for Submm Integrated Receiver

V.P. Koshelets[1,3], S.V. Shitov[1,3], L.V.Filippenko[1], P.N. Dmitriev[1], A.B. Ermakov[1,3], A.S. Sobolev[1], M.Yu. Torgashin[1], A.L. Pankratov[2], V.V. Kurin[2], P. Yagoubov[3], R. Hoogeveen[3]

[1]Institute of Radio Engineering and Electronics (IREE), Moscow, Russia

[2]Institute for Physics of Microstructure (IPM), Nizhny Novgorod, Russia

[3]National Institute for Space Research (SRON), the Netherlands

Abstract. Comprehensive measurements of the FFO radiation linewidth are performed using an integrated harmonic SIS mixer; the FFO linewidth and spectral line profile is compared to a theory. Essential dependence of the FFO linewidth on frequency is found; possible explanation is proposed. The results of numerical solution of the perturbed sine-Gordon equation qualitatively confirm this assumption. To optimize the FFO design, influence of the FFO parameters on the radiation linewidth is studied. Novel FFO design at a moderate current density has resulted in a free-running FFO linewidth of about 10 MHz in the flux flow regime up to 712 GHz being limited only by the gap frequency of Nb. This relatively narrow free-running linewidth (along with implementation of a wide-band phase locking loop system) allows continuous phase locking of the FFO in the wide frequency range of 500 – 710 GHz. These results are the basis for the development of 550-650 GHz integrated receiver for the Terahertz Limb Sounder (TELIS) intended for atmosphere study and scheduled to fly on a balloon in 2005. We report here also on the design of the second generation of the phase-locked SIR chip for TELIS.

1. Introduction

Presently a Josephson Flux Flow Oscillator (FFO) [1] appears to be the most developed superconducting local oscillator for integration with an SIS mixer in a single-chip submm-wave receiver [2]. Superconducting Integrated Receiver (SIR) [2] comprises in one chip a planar antenna and an SIS mixer, pumped by an integrated superconducting local oscillator (LO). The concept of an SIR has been experimentally proven: a DSB receiver noise temperature below 100 K has been demonstrated around 500 GHz; a compact imaging array of nine SIRs has been developed and tested [2, 3]. The frequency resolution of a heterodyne spectrometer is one of the major parameters for a practical application. In order to obtain the required resolution (of at least one part per million) the local oscillator must be phase-locked to an external reference. To ensure the phase locking, the free-running linewidth of the FFO has to be well below an effective regulation bandwidth of the PLL (of about 10 MHz).

Detailed measurements of the FFO linewidth were performed in a wide frequency range up to 700 GHz using a novel experimental technique based on an integrated harmonic mixer [4]. A Lorentzian shape of the FFO line has been observed both at higher voltages on the flux flow step (FFS) and at lower voltages on the Fiske steps (FS's) [5] in the resonant regime. It means that the free-running ("natural") FFO linewidth in all operational regimes is determined by the wideband thermal fluctuations and the shot noise. This is different from many traditional microwave oscillators where the "natural" linewidth is very small and the observed linewidth can be attributed mainly to external fluctuations. It was found that free-running FFO linewidth exceed theoretical estimations made for lumped tunnel Josephson junction. To explain the experimentally measured dependence of the FFO linewidth, an additional term proportional to differential resistance on control line current (producing magnetic field for the FFO operation) has been introduced to the noise model of FFO [5 - 7]. Recently a physical reason for such additional term has been proposed [8]. The solution is based on the assumption that part of the DC bias current creates an additional magnetic field in the junction.

In this report the results of the comprehensive study of the dependence of the FFO linewidth on voltage (FFO frequency), current density and the FFO geometry are presented. Part 3 of the paper is devoted to the design and test results of the SIR with phase locked FFO designed for TELIS.

2. FFO linewidth; dependence of the FFO frequency and current density.

Experimentally measured dependences of the FFO linewidth are presented in Fig. 1 for junctions with uniform bias current distribution (without "unbiased tail"). Abrupt increase of the linewidth at the FFO frequency of about 450 GHz is caused by the effect of Josephson self-coupling (JSC) [9, 10], which considerably modifies the FFO properties at voltages $V \approx V_{JSC} = 1/3*V_{gap}$ (V_{JSC} corresponds to 450 GHz for a Nb-AlO_x-Nb FFO). The increase of the intrinsic FFO linewidth due to the larger internal damping caused by JSC effect at voltages $V > V_{JSC}$ significantly complicates phase locking of the FFO.

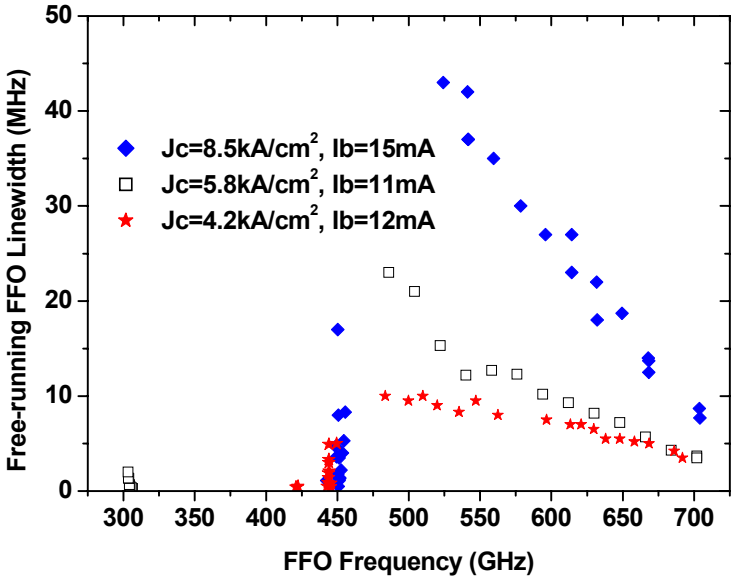

Figure 1. Dependence of the FFO linewidth on oscillation frequency measured for FFOs of the same design, but fabricated from three trilayers with different current densities, J_c. The linewidth is measured at constant bias current, while the FFO frequency (voltage) is tuned by the magnetic field (by the control line current).

For all current densities there is a well-defined dependence of the free-running FFO linewidth on frequency (voltage). In the model [5, 6] a direct voltage dependence of the FFO linewidth is negligibly small. Since the data are taken at a constant bias current, the variation of the linewidth on the bias voltage can be mainly attributed to changes in the differential resistance. Indeed, data on Fig. 2 demonstrate such dependence (see also [11]); it is observed for all tested FFOs of very different designs. Presumably it reflects the fact that introduction of an additional fluxon into the junction requires a larger control line current as the fluxon chain gets denser. This assumption is confirmed by numerical calculations (see Fig. 3).

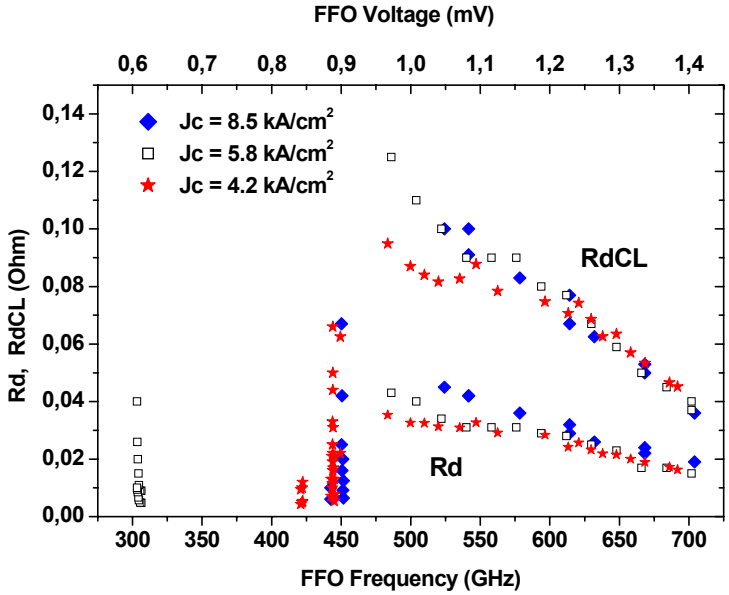

Figure 2. Differential resistances on bias current, R_d, and magnetic field (control line current), R_d^{CL}. Differential resistances are calculated from the voltage change ΔV found at small increment of two currents ΔI and ΔI_{cl}, respectively. The voltage change ΔV is determined by measuring the frequency of the emitted radiation.

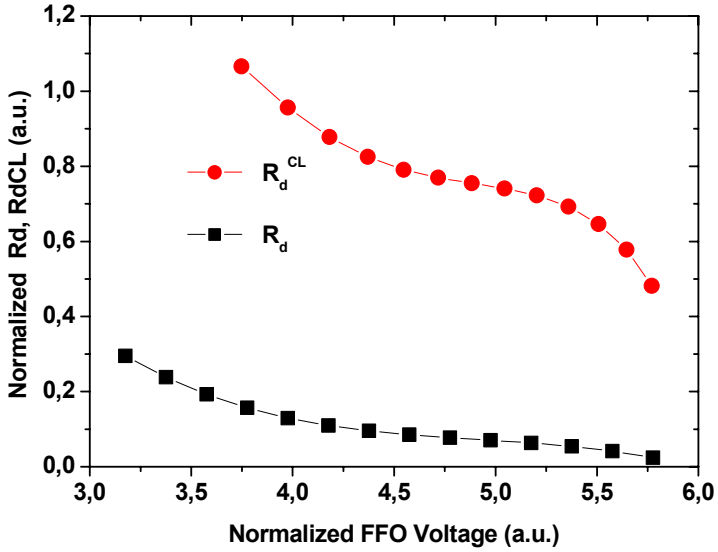

Figure 3. Differential resistances R_d and R_d^{CL} calculated at the normalized bias current 0.3 for the junction length l = 40 and damping $\alpha = 0.05$.

The differential resistances for Fig.2 were obtained during FFO linewidth measurements what enables measurement of voltage increments with accuracy better than 20 nV by observing the frequency change of the emitted radiation. Note, that the results of direct DC measurements (which average data in the range of about 1-2 μV) give exactly the same dependence. It should also be mentioned that R_d and R_d^{CL} are bounded: their ratio is almost constant over the wide voltage range. The details of this study will be published elsewhere.

The results of numerical solution of the perturbed sine-Gordon equation are presented in Fig. 3. The dimensionless parameters are chosen to be close to the experimental ones: the length (normalized on Josephson penetration depth) $l = 40$, the damping $\alpha = 0.05$, the magnetic field varies from 3 to 8 (flux flow step). As it is seen from Fig. 3 both R_d^{CL} and R_d decrease with the increase of the voltage.

Data presented in Fig. 1 demonstrate also a considerable increase of the FFO linewidth with FFO current density. Note that bias currents for all current densities are quite similar and their difference cannot explain the existing broadening of the FFO linewidth. Again, the increase is mainly caused by changing of the differential resistance. That is confirmed by data presented in Fig. 4, where the experimental linewidth is normalized on theoretically calculated linewidth values. The linear fits to the normalized data coincide well with each other (and with unity line) for all current densities. It proves that an additional broadening discussed in the papers [12, 13] does not play a significant role for present FFO parameters and the linewidth can be precisely calculated using the developed FFO model [5 - 7]. Note that experimentally determined values of the coefficient K, are used for calculation of the FFO linewidth. This coefficient accounts for the influence of the magnetic field created by the bias current [8] by adding the product $K*R_d^{CL}$ to the measured R_d. The K-value varies from 0.35 (at small bias currents near the quasiparticle curve) down to zero (at the end of flux-flow step) for FFO without "unbiased tail".

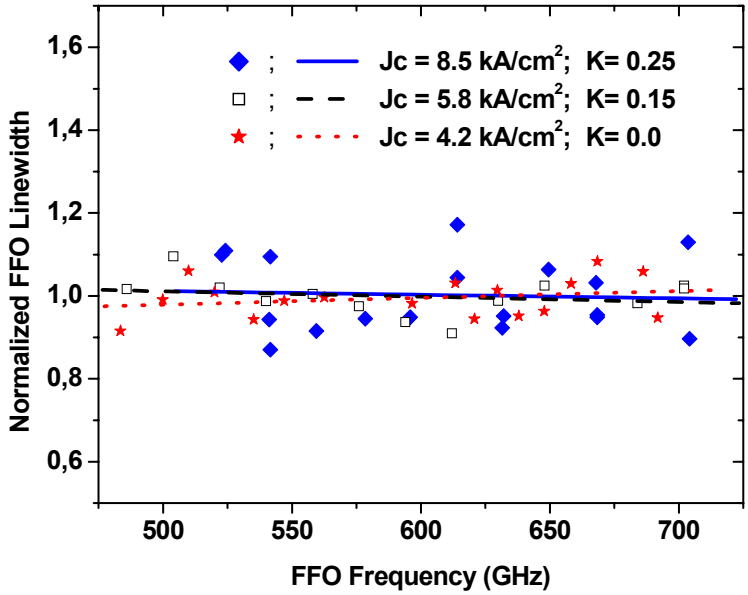

Figure 4. Experimental linewidth normalized on theoretical values. Calculations are based on the FFO model [5, 6] using experimentally measured values of differential resistances and currents. Linear fits to the normalised data are shown by appropriate lines.

It has to be noted that high current density ($J_c \geq 8$ kA/cm^2) is important for wide-band operation of an SIS mixer at submillimeter wave range. It is found that increase of the current density leads to the growth of the differential resistances (instead of expected decrease!) that creates serious problem in design and development of SIR chips. Implementation of two separate trilayes with different current densities for the SIS mixer (high J_c) and for the FFO (lower J_c) might be the solution.

To study a dependence of the FFO linewidth on the profile of the bias current, we fabricated a set of FFOs with different number of separate bias "fingers". The FFO junction itself (i.e. tunnel layer area) is exactly the same as in previous experiments (Fig. 1, 2), only the geometry of the top electrode is changed. Each "finger" (width - 4 μm, separation between fingers – 16 μm) includes a small series resistor to provide a uniform current distribution. Our measurements demonstrate that design with separate fingers results in a much wider FFO linewidth (see Fig. 5 - diamonds). For an FFO with unbiased tail (several fingers from the "input" end of the FFO are removed) linewidth becomes smaller, approaching the data for traditional design, which can be described as one broad electrode, not divided into the "fingers". These data demonstrates that a linewidth of the oscillator is mainly determined by the current distribution at the "input" end of the FFO. Possible reasons for essential increasing of the FFO linewidth for biasing scheme with separate fingers might be: a) spatial modulation of the bias current, b) extra noise generated by bias resistors. Additional studies are required for optimization of the FFO design for TELIS.

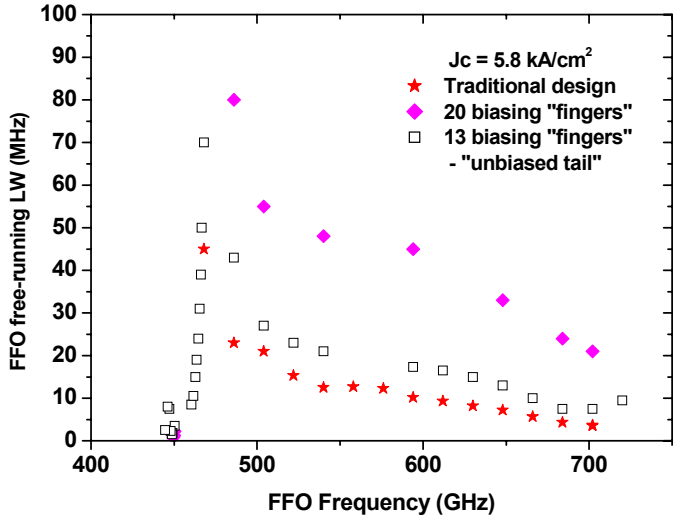

Figure 5. Experimental linewidth measured for FFO of different design.

3. Design and test of the phase-locked SIR

In order to resolve a weak signal adjacent to a strong spectral line, a local oscillator of a heterodyne spectrometer (PL FFO) must have a well-defined (narrow) line-shape. The dynamic range of the spectrometer is closely related to the ratio between the carrier and the spectral power density (FFO phase noise) at a frequency offset equivalent to the channel spacing of the spectrometer. The phase noise of the phase-locked FFO of about -80 dBc/Hz at the 1 MHz offset from the carrier has been reported at 700 GHz [14]. For the 1 MHz channel one may expect a dynamic range of 20 dB for the spectrometer that satisfies requirements for single dish radio astronomy and atmospheric monitoring. For comparison, this figure fits well requirements for the wide-band spectrometer of HIFI instrument of Herschel Space Observatory prepared for launch in 2007.

We have demonstrated experimentally for the first time a sensitive heterodyne spectrometer employing a superconducting local oscillator at 327 GHz [15]. A breadboard of a superconducting integrated spectrometer with the phase-locked FFO has been tested showing the frequency resolution of the receiver as good as 10 kHz. The effect of broadening of a spectral line of SO_2 gas at 326867 MHz was measured by this spectrometer for a laboratory gas cell within the pressure range of 0.03-0.3 mbar demonstrating the feasibility of such device for practical applications.

Here we report on the first results of design and test of the phase-locked SIR for TELIS. The device comprises a double-dipole lens-antenna SIS-mixer pumped by an integrated FFO. The FFO provides the rf power also for the harmonic mixer integrated on the same silicon chip of size 4 mm x 4 mm x 0.3 mm; this harmonic mixer is a part of the FFO phase locking loop. Since the advantage of the SIR technology is the wide-band tuneability of the integrated FFO, we are developing a new wide-band device with an instantaneous bandwidth of 500-650 GHz emphasizing the 600-650 GHz frequency range. This enables covering the wide range of atmospheric species responsible for ozone depletion. A few new solutions are implemented in the SIR chip making it a new generation. To achieve the wide-band performance of the spectrometer, a side-feed twin-SIS mixer with 0.8 μm^2 junctions integrated with a double-dipole antenna is used. To minimize the magnetic field interference to the FFO, the control line of the SIS mixer (the integrated magnetic coil) is folded and placed opposite to the FFO, resulting in a 10^{-3} suppression coefficient.

A few batches have already been produced at IREE and preliminary tested at SRON at dc and with a Fourier transform spectrometer (FTS). The FTS test presented in Fig. 6 demonstrates a possibility to obtain the wide instantaneous bandwidth for the double-dipole twin-SIS mixer. However, we did not succeed yet in getting precise wide-band and low-loss coupling over the complete band. The fit demonstrated in Fig. 6 is only a qualitative one. Analyzing the experimental data, we have found that accurate EM simulation of the antenna structure is required. A few important results are obtained recently via development of proper EM-models for the key elements of the circuit that is a good basis for further improvement of the complex SIR device. A heterodyne test is under preparation.

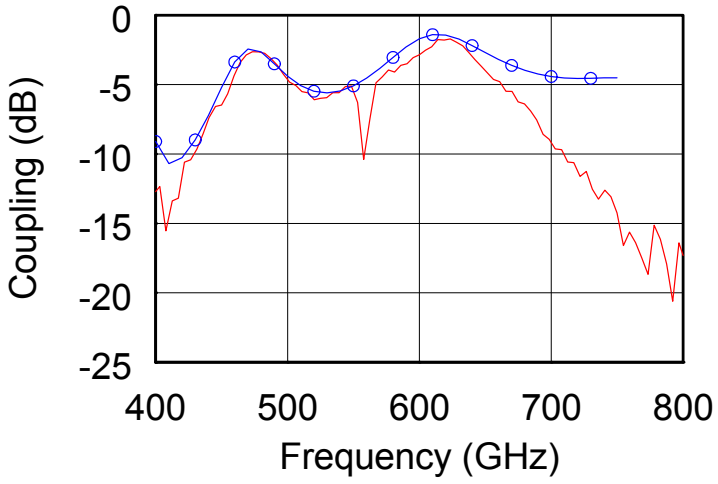

Figure 6. Experimental FTS data (solid) and simulated fit (smooth curve marked by circles) for signal coupling for twin-SIS double-dipole mixer. The increasing discrepancy above 670 GHz is caused by dissipative loss above gap frequency of Nb.

The work was supported in parts by RFBR (projects 03-02-16748, 02-02-16775, 03-02-16533, 03-02-06343, 03-02-06683), by INTAS (project 01-0367, 01-0450) and by ISTC project 2445.

References

[1] Nagatsuma T, Enpuku K, Irie F, and Yoshida K 1983 *J. Appl. Phys.* **54** 3302-3309, see also Pt. II: 1984 *J. Appl. Phys.* **56** 3284; Pt. III: 1985 *J. Appl. Phys*. **58** 441; Pt. IV: 1988 *J. Appl. Phys.* **63** 1130

[2] Koshelets V P and Shitov S V 2000 Superconductor Science and Technology **13** R53-R69

[3] Shitov S V, Koshelets V P, Ermakov A B, Filippenko L V, Baryshev A M, Luinge W, Gao J - R 1999 *IEEE Trans. Appl. Supercond.* **9** 3773-3776

[4] Koshelets V P, Shitov S V, Filippenko L V, Shchukin A V, Mygind J 1996 *Appl Phys Lett* **69** 699-701

[5] Koshelets V P, Ermakov A B, Dmitriev P N, Sobolev A S, Baryshev A M, Wesselius P R, Mygind J 2001 *Superconductor Science and Technology* **14** 1040-1043

[6] Koshelets V P, Dmitriev P N, Sobolev A S, Khodos V V, Pankratov A L, Vaks V L, Baryshev A M, Wesselius P R , Mygind J 2002 *Physica C* **372–376** 316–321

[7] Pankratov A L 2002 Physical Review B **65** 054504-1-9.

[8] Mygind J, Mahaini C, Samuelsen M R, Sobolev A S, Torgashin M Y, Koshelets V P Spectral Linewidth of Josephson Flux Flow Oscillators; influence from bias and geometry, this conference, Report 819.

[9] Hasselberg L - E, Levinsen M T and Samuelsen M R 1974 *Phys Rev B* **9** 3757-3765.

[10] Koshelets V P, Shitov S V, Shchukin A V, Filippenko L V, Mygind J, and Ustinov A V 1997 *Phys Rev B* **56** 5572-5577

[11] Koshelets V P, Shitov S V, Dmitriev P N, Ermakov A B, Sobolev A S, Torgashin M Yu, Wesselius P R, Yagoubov P A, Mahaini C, Mygind J 2003 *IEEE Transactions. on Applied Superconductivity* **13-**2 *1035-1038*

[12] Golubov A A, Malomed B A, Ustinov A V 1996 *Phys Rev B* **54** 3047

[13] Betenev A P and Kurin V V 1997 *Phys Rev B* **56** 7855

[14] Koshelets V P, Dmitriev P N, Ermakov A B, Sobolev A S, Torgashin M Yu, Khodos V V, Vaks V L,Wesselius P R, Mahaini C, Mygind J 2002 Proceedings of the 13-th International Symposium on Space Terahertz Technology (Harvard University) 473-482

[15] Shitov S V, Koshelets V P, Ermakov A B, Dmitriev P N, Filippenko L V, Khodos V V, Vaks V L, Yagoubov P A, Vreeling W - J and Wesselius P R 2003 *IEEE Transactions on Applied Superconductivity* **13-**2 *684-687*